Courtship song differs between African and European populations of *Drosophila melanogaster* and involves a strong effect locus

Matthew J. Lollar[1,@], Elizabeth Kim[2], David L. Stern[2], John E. Pool[1,@]

[1]Laboratory of Genetics, University of Wisconsin – Madison, Madison, WI, 53705, USA

[2]Janelia Research Campus, Howard Hughes Medical Institute, Ashburn, VA, 20147 USA

Corresponding author contact: mjlollar1@gmail.com; jpool@wisc.edu

Running head: Genetics of song evolution within *D. melanogaster*

Keywords: courtship song, behavior, QTL mapping, variation, evolution

ABSTRACT

The courtship song of *Drosophila melanogaster* has long served as an excellent model system for studies of animal communication and differences in courtship song have been demonstrated among populations and between species. Here, we report that flies of African and European origin, which diverged approximately 13,000 years ago, show significant genetic differentiation in the use of slow versus fast pulse song. Using a combination of quantitative trait mapping and population genetic analysis we detected a single strong QTL underlying this trait and we identified candidate genes that may contribute to the evolution of this trait. Song trait variation between parental strains of our recombinant inbred panel enabled detection of genomic intervals associated with six additional song traits, some of which include known courtship-related genes. These findings improve the prospects for further genetic insights into the evolution of reproductive behavior and the biology underlying courtship song.

INTRODUCTION

Communication, the process of information transfer through signal production and recognition, is abundant across the animal kingdom. There are many forms of communication in nature, from chemical interactions between bacteria (Keller & Surette 2006), to intricate mating displays of suboscine passerines (Prum 1990), or the complexity of human language (Lieberman 1971). Accompanying this diversity of form is a diversity of purpose: communication is used by animals in mate choice and conspecific recognition (Anholt *et al.* 2020), antagonistic displays (Maynard Smith 1979), and cooperative behavior such as territory defense and foraging (Fitzgerald & Peterson 1988). Often, the proper transmission of information from signaler to receiver has important consequences for the fitness and reproductive success of an individual (Maynard Smith 1979; Anholt *et al.* 2020), underpinning its importance in both standing diversity and the evolutionary history of populations. Acoustic communication has evolved independently over 20 times across insects (Greenfield 2016) and is an important component of reproductive behavior (Leonhardt *et al.* 2016).

Male *Drosophila melanogaster* “sing” to females by vibrating their wings, typically as unilateral extension of a single outstretched wing (Ewing & Bennet-Clark 1968). In *D. melanogaster*, song consists of two primary modes: a series of continuous sinusoidal waves or hums (sine song) and trains of more punctuated wave clusters (pulse song) with amplitude and pitch typically exceeding those produced by sine song (Swain & Philipsborn 2021). Furthermore, two modes of pulse song have been identified based on the pitch of the pulse song: fast and slow pulse modes (Clemens *et al.* 2018). Female

Drosophila typically become more receptive to mating upon hearing song (von Schilcher 1976) and may distinguish between subtle differences in song components. The active female responses to courtship that encourage or discourage copulation underpin the role of song in the reproductive success of male flies (Cook 1973; Riabinina *et al*. 2011; Laturney & Moehring 2012).

Male courtship song has been characterized in many *Drosophila* species, (O'Grady & DeSalle 2018), providing deep historical knowledge in a system benefiting from excellent genetic tractability (St. Johnston 2002; *Drosophila* 12 Genomes Consortium 2007). The acoustic properties of pulse song, such as the interpulse interval (IPI) typically receive the greatest attention (Ritchie *et al.* 1994; Talyn & Dowse 2004; Stern 2014), although components of sine song also vary among closely related species (Ding *et al.* 2016). Pulse song is highly variable across species and has been implicated in mate and conspecific recognition (Spieth 1952; Bennet-Clark & Ewing 1969; Watanabe & Kawanishi 1979; Cowling & Burnet 1981; Talyn & Dowse 2004; Ding *et al.* 2019), although song does not appear to contribute to mate choice in every species (Richie *et al.* 1999; Iglesias & Hasson 2017).

The genetic architectures and underpinnings of variation in courtship song and other premating isolating mechanisms are poorly understood. Early studies supported the view that variation in these behaviors was caused by a small number of loci of large effect (Mackay 2001; Mackay *et al.* 2005). Arbuthnott (2009) found, for instance, that among 36 studies in insects (predominantly *Drosophila)* on courtship traits contributing to premating

isolating barriers, 25 studies considered traits to be influenced by a few loci of large effect. However, quantitative trait locus (QTL) studies are likely biased toward detecting large effect loci (Rockman 2012). More recent studies have revealed that the genetic architecture of premating barriers is likely more complex (Mackay 2009; Arbuthnott 2009; Oh *et al*. 2012; Shahandeh & Turner 2020). The number of loci contributing to variation in a trait involved in premating isolation can also have implications for the rate of speciation between species (Gavrilets & Vose 2007), providing additional incentive to study the evolution of such phenotypes.

Differences between well-isolated species in reproductive behavior may or may not have contributed to the initial reproductive isolation of those species (Price 2002). On the other hand, within-population variation in such traits may be distinct in its genetic architecture and basis from evolutionary trait changes (Arbuthnott 2009). Whereas, evolved differences in courtship traits between interfertile taxa, including recently diverged populations of the same species, may hold particular interest for the study of reproductive isolation.

D. melanogaster originated in sub-Saharan Africa and has spread nearly worldwide (Lachaise & Silvain 2004, Lachaise *et al.* 1988, Keller 2007). The demographic history of the species is well-studied (e.g. Sprengelmeyer *et al.* 2020) and striking genetic and phenotypic changes have occurred on a relatively short evolutionary time-scale. Genetic differentiation is in part due to at least one moderate population bottleneck during the initial migration out of sub-Saharan Africa (Begun & Aquadro 1993, Sprengelmeyer *et al.*

2020), as well as locally adaptive changes in response to novel environmental pressures (David & Capy 1988, Fabian *et al.* 2015; Lack *et al.* 2016a). Genes under selection as a consequence of adaptation often have neuronal or morphological and developmental functions (Fabian *et al.* 2015; Lack *et al.* 2016a; Pool *et al.* 2017). Such changes could have either specific or pleiotropic effects on courtship traits such as song, in light of the multifaceted roles of many genes involved in courtship behavior (Gleason 2005; Greenspan & Ferveur 2000).

While some components of courtship song variation within *D. melanogaster* have been studied (Colegrave *et al.* 1999; Gleason *et al.* 2002), there have been no prior comprehensive intraspecific studies of many courtship song components. Here, we utilize panels of naturally-derived *D. melanogaster* from two geographic origins, Zambia and France, and high-throughput methods of recording and analyzing courtship song (Arthur *et al.* 2013; Arthur *et al.* 2021) to study the genetic basis of song differences between populations. We find that the proportion of slow and fast pulses (“pulse mode preference”) differs significantly between populations. We use a panel of recombinant inbred lines (RILs) derived from reciprocal crosses between France and Zambia strains to map pulse mode preference as a quantitative trait, as well as mapping eight additional song traits that differ significantly between RIL parental strains. Finally we complement our mapping analysis with population genetic screens across QTL intervals, highlighting the most genetically differentiated loci between populations to identify additional genes that may underline song variation and evolution. Collectively, our results reveal that naturally evolved differences in male song components exist between populations within the *D.*

120 *melanogaster* species and include moderately strong effect loci, opening the door to
121 targeted genetic and neurophysiological studies of their molecular basis.
122

123 MATERIALS AND METHODS

124 *Drosophila husbandry and stocks*

125 Two distinct types of strains were used in this study. Strains used to measure trait
126 differences between population samples were (8 generation) inbred lines from wild-
127 derived isofemale stocks, collected at locations described in Pool *et al.* (2012). We used
128 a recombinant inbred line (RIL) panel generated in the lab and derived from a reciprocal
129 cross between two inbred strains, one each from our France (FR) and Zambia (ZI)
130 collections (FR320N and ZI418N), for QTL mapping. Following 12 generations of
131 intercrossing, isofemale lines were established from these interbred flies and inbred for 5
132 generations to establish the final panel, from which 305 recombinant strains were
133 included in the present study. Females used in mating assays were derived from a single
134 France strain, FR54N. We chose this strain because European females show less
135 preference across populations compared to some southern African strains (Grillet *et al*.
136 2012; Hollocher & Wu, 1996; Wu *et al*. 1995), who tend to disfavor non-African males,
137 and female response can influence the expression of song (Riabinina *et al*. 2011;
138 Laturney & Moehring 2012).
139

140 Flies were maintained as stocks in laboratory conditions on food prepared in batches of
141 4.5 L water, 500 mL cornmeal, 500 mL molasses, 200 mL yeast, 54 g agar, 20 mL
142 propionic acid, and 45 mL tegosept 10% (in 95% ethanol). Flies used in assays were

collected under carbon dioxide anesthesia and aged in one of two 12 hour light/dark controlled incubators, separated in cycle by two hours to allow additional assays each day. Incubator temperatures were not strictly controlled but measured daily and ranged from 23-25C. Females were collected and aged in plastic fly food bottles containing approximately 50 females per bottle. Males were collected and aged individually in glass fly food vials. The age of collected males ranged from 0-24 hours post-eclosion and was not strictly controlled for prior matings during this time. Previous matings can affect male mating success (e.g. Sinclair *et al*. 2021), although the frequency of matings among our males may have been low due to the 0-24 hours age range of the females (Manning 1967). Whereas, prior courtship attempts may have been more variable among the collected males, given that males begin to court as early as 12 hours post-eclosion (Strömnæs & Kvelland 1962) and may court virgin females (Dukas 2005). The collection of tens of males from each fly strain (see below), and the averaging of their song trait values, should dampen individual-level variation induced by such factors.

Song recording

Male song was recorded on a multi-channel acoustic recording chamber (Arthur *et al*. 2013), at Janelia Research Campus from June-July of 2022 (Table S1). Males used in assays were collected 0-24 hours post-eclosion, isolated into individual vials, and aged for 3-5 days. Males were recorded in the presence of a single unmated female, collected 0-6 hours post-eclosion, and aged an additional 12-24 hours before use in assays. This age was selected as an optimal range to allow aging of females past a “young nymph” stage, without allowing them to become old enough to be receptive to mating (Manning

166 1967), which would diminish the duration of captured song before copulation
167 (observationally, males that initiated song typically sang throughout the entire duration of
168 recording if they did not mount successfully). Flies were mouth aspirated into recording
169 chambers, and assays were performed within the first two hours from lights on. Male flies
170 were recorded for a consecutive duration of 30 minutes. Replicate assays were performed
171 such that strains were assayed in sets of 6-8 males across 3-5 unique days, for a total
172 target sample size of 24 for each RIL, and 50-60 for each inbred strain (Table S1).
173
174 *Song analysis and software protocols*
175 Song data was automatically segmented and analyzed without human intervention using
176 SongExplorer (doi:10.1101/2021.03.26.437280) to annotate acoustic components of
177 song. A previously trained *D.melanogaster* model detected four principle sounds (sine
178 song, pulse song, ambient noise, other), trained using audio collected on the recording
179 instrumentation used in this study. Samples were recorded at a sampling rate twice that
180 of the provided model, so raw audio files were downsampled at a rate of one half using
181 the “signal” function in the python open-source package SciPy (version 1.13) for proper
182 segmentation (Virtanen *et al.* 2020).
183
184 Segmented song parameters were quantified using BatchSongAnalysis
185 (https://github.com/dstern/BatchSongAnalysis) with small modifications for individualized
186 trait parameterization (https://github.com/mjlollar/song_work), MATLAB version 9.13
187 (R2022b) (The MathWorks Inc. 2022). The numbers of song bouts, sine and pulse song
188 durations, interpulse interval characteristics, pulse/sine carrier frequencies and pulse/sine

train lengths were measured as described in Arthur *et al.* (2013). Pulse and sine song amplitude were measured by calculating the square root of the mean of the squares of all pulses in a song (output as arbitrary units). Transition probabilities were calculated using the Matlab “transProb()” function for pairwise measurements of events (The MathWorks Inc. 2022). Slow and fast pulse characterization was available thanks to previous classification training in the model provided and used methods similar to those described in Clemens *et al.* (2018) to differentiate and classify pulse modes. Interpulse intervals were estimated independently of pulse carrier frequency by fitting an envelope to each pulse to estimate pulse duration and calculating the interpulse interval as the time from the end of one pulse to the center of the next pulse. Here, pulse event carrier frequency was measured as the modal frequency detected by SongExplorer. Further discussion on the characterization of carrier frequency can be found in Ding *et al.* (2019).

Replicates with fewer than one second of song per minute, or those with an aberrantly high sine song rate per minute (recordings with >55 seconds of characterized sine song appeared to represent a failure of recording equipment) were excluded from analysis. Additionally, replicates with zero values for a trait were not considered when calculating strain mean for that trait, as a zero value from BatchSongAnalysis was typically the result of an inability to properly measure trait values (due to minimal sampling throughout the assay, etc.). Trait values for strains were represented as the mean value of the total remaining replicates.

211 Prior to filtering, the number of replicate inbred and RIL samples totaled 860 and 7,152,
212 respectively. After the filtering described above was applied to raw data, the total number
213 of inbred song recordings were 810, with an average replicate number of about 43
214 recordings per strain. The total number of RIL song recordings totaled 5,532 after filtering,
215 with an average of about 19 recordings per RIL line.
216
217 *Data analysis of processed song recordings*
218 Differences in the population mean trait values were quantified for each trait using Mann-
219 Whitney (MW) tests using the two-sample wilcox.test() function in R (R Core Team 2023;
220 https://github.com/mjlollar/song_work). To statistically control the testing of multiple traits,
221 we used a permutation-based approach to correct for multiple testing that accounted for
222 non-independence among some traits (Figure S1). 10000 permutations were performed
223 in the following design. For each replicate, the identities of each strain were randomly
224 shuffled and drawn without replacement to represent 10 FR strains and 7 ZI strains
225 (matching sample sizes of the empirical data). MW tests were calculated between these
226 groups and recorded. We then determined the false positive rate (the likelihood the
227 empirical MW p-value occurs by chance) as the proportion of permutation replicates that
228 gave a p-value as low or lower than the empirical value. Correlation statistics were
229 generated in R using Pearson's test (R Core Team 2023).
230
231 For a trait showing evidence of population differentiation from the above methodology,
232 we also calculated Q_{ST} as a measure of quantitative trait differentiation (Lande 1992;
233 Spitze 1993). To indicate whether this trait might fall outside the range of neutral

234 population differentiation, we compared the estimated Q_{ST} to the distribution of F_{ST} at
235 individual SNPs (which conservatively maximizes the variance of F_{ST}), calculated from
236 allelic sample sizes identical to the number of strains from which phenotypic data was
237 obtained. F_{ST} distributions were calculated using available genomes from the *Drosophila*
238 Genome Nexus (Lack *et al*. 2016a; see below).
239
240 *QTL mapping based on RIL ancestries*
241 Genomic sequencing of the RIL panel is described in da Silva Ribeiro *et al.* (2024), which
242 also documents the calling of parental strain ancestry. Briefly, for each RIL, homozygous
243 and heterozygous parental strain ancestry calls were assigned using Ancestry HMM
244 (Corbett-Detig & Nielsen 2017) on windows defined by intervals containing 2,500 SNP
245 genotype differences between the two parental strains (which were used as the parental
246 panels for Ancestry HMM). This window size provides an abundance of variants from
247 which to infer ancestry in any particular window, but given that they average 5 kb in length,
248 they are still much smaller than the typical expected length of ancestry tracts, which
249 should tend to be roughly on the megabase scale after 12 generations of interbreeding.
250
251 QTL mapping was performed using parental strain ancestry calls as marker genotypes.
252 We used a modified version of r/QTL (Broman *et al*. 2003) that allowed us to use an
253 additive QTL model, rather than allowing each genotypic class to have an independent
254 mean trait value (da Silva Ribeiro *et al.* 2024), in light of the smaller counts of some
255 ancestry genotypes observed in many genomic windows. The primary model tests the
256 alternative hypothesis of a single QTL against the null hypothesis of no QTL, while using

257 phenotypic permutations (n=10,000) to control for genome-wide multiple testing. More
258 explicit details of the pipeline can be found in da Silva Ribeiro *et al.* (2024), as well as
259 source code at https://github.com/ribeirots/RILepi. We note that this permutation
260 approach, along with the averaging of multiple individual trait values per RIL, should
261 minimize the potential influence of skewed trait distributions on our QTL mapping.
262
263 The above analysis yields a genomic LOD score landscape for any given song trait.
264 However, when this landscape is complex or ragged in its topography, in practice it can
265 be difficult to assess which local peaks to consider as distinct QTLs. We therefore
266 implemented a series of criteria to determine which local peaks to integrate into the same
267 QTL region, and also to denote which regions within a broad/complex QTL may have the
268 greatest likelihood of containing a causative locus. Preliminary QTL peak regions were
269 defined based on contiguous runs of windows above the genome-wide LOD significance
270 threshold. A pair of initially separate peaks separated by a valley with a minimum LOD
271 value of greater than the shorter peak's maximum LOD score minus 1.5 were merged
272 into the same peak region – since a simple confidence interval (CI) for the shorter peak,
273 based on a 1.5 LOD drop, would end up including the taller peak. After defining and
274 integrating peaks in this manner, we accounted for peaks with complex LOD landscapes
275 by differentiating between "inclusive" and "restrictive" CIs. Within a contiguous run of
276 windows above the LOD significance threshold, the inclusive CI was defined as the full
277 span encompassing all local windows in which the local LOD score was greater than the
278 region's maximum LOD score minus 1.5. A QTL region's inclusive CI was therefore

contiguous by definition, and could encompass some windows with LOD scores less than the maximum LOD minus 1.5.

In contrast, restrictive Cis were defined as only the subset of windows within the inclusive CI that had LOD scores greater than the maximum LOD minus 1.5 (https://github.com/mjlollar/song_work). A QTL region's restrictive CI could therefore encompass multiple non-contiguous runs of windows representing different LOD sub-peaks within the same QTL region as defined above. Based on the LOD scores of their constituent windows, restrictive Cis were considered to be the most likely intervals to contain a causative locus, and were therefore the focus of downstream analysis as described below. Windows yielding a RIL panel-wide ancestry proportion above 90% for either parental strain were excluded from the mapping analysis, and confidence intervals (Cis) encountering such regions were extended until encountering an included window that ended the CI based on the criteria detailed above.

Residual Mapping of Correlated Traits

In cases where we separately performed QTL mapping on two correlated traits, we investigated whether overlapping QTL might reflect pleiotropic effects of a single locus. We performed a limited set of residual trait mapping analyses using linear regression to find each RIL's residual trait values for the second trait after adjusting for its observed value for the first trait (here, treating the trait with the greater QTL LOD score as the first trait). QTLs and confidence intervals were identified using identical methods described in

301 the previous sections. Linear regression was performed in python using the SciPy
302 *linregress* package.
303
304 *Population Genetic and Candidate Gene Analysis of QTL regions*
305 Previous population genomic data available from the *Drosophila* Genome Nexus (Lack *et*
306 *al.* 2016a) was used to generate a population genetics database. We used all available
307 Zambia and France genomes for a total of 197 and 96 strains, respectively. Under the
308 hypothesis that the two population-differentiated song traits may have been influenced by
309 population-specific selection, we assessed three window-based population genetic
310 statistics across the restrictive Cis of each QTL region for those traits: 1) $F_{ST_FullWin,}$ which
311 represents the estimated F_{ST} value of a window using all variable sites within the window;
312 2) F_{ST_MaxSNP}, the maximum F_{ST} value of any variable site within a window (da Silva
313 Ribeiro *et al.* 2022); and 3) Comparative Haplotype Identity (χ_{MD}), which tests for evidence
314 of local adaptation by comparing the summed lengths of pairwise identical haplotypes
315 within one population versus another (Lange & Pool 2016).
316
317 We then identified “candidate genes” within QTL Cis (using the restrictive CI definition
318 above, including only the windows within an extended CI that had LOD scores greater
319 than the peak value minus 1.5). We associated genes with windows if any of their exons
320 (coding or non-coding) overlapped a given window, or if an exon of this gene was the first
321 exon to the left or right of this window’s boundaries (in order to account for potential
322 regulatory regions of a given gene). We included as candidates any genes that had been
323 previously implicated in courtship behavior. A list of 92 such genes was generated using

genes sourced from the Gene Ontology (GO) database category “male mating behavior” (ID GO:0060179) as well as additional genes identified from cursory literature searches (Table S2).

For traits with evidence of population differentiation, we additionally included as candidates genes with a documented role in wing development or the nervous system. Wing genes included the GO categories “wing disc development” (GO:0035220) and “wing disc morphogenesis” (GO:0007472), for a total of 743 genes. Neuronal genes included the GO categories “nervous system development” (GO:0007399) and “nervous system process” (GO:0050877), for a total of 1,810 genes. For these same differentiated traits, we also annotated genes with evidence for local adaptation, in that they were associated with at least one window that fell within the top 1% quantile of values for either $F_{ST_FullWin}$, F_{ST_MaxSNP}, or X_{MD}. A gene was considered to be associated with an outlier window if at least one of its coding exons overlapped the window boundaries or represented the nearest neighboring exon (in either direction).

339 RESULTS

340 *AFRICAN AND EUROPEAN POPULATIONS OF* D. MELANOGASTER *MAY DIFFER IN*
341 *MULTIPLE COMPONENTS OF PULSE SONG*

342 We first sought to determine whether any quantitative aspects of male courtship song
343 varied between two *D. melanogaster* populations: one from within the species' inferred
344 ancestral range (Siavonga, Zambia) and one from Europe (Lyon, France). We divided
345 components of male song into a range of acoustic properties, each considered as a single
346 quantitative trait. To first identify population-level differences in specific song traits, we
347 selected 10 France-derived and 7 Zambia-derived inversion-free inbred strains from
348 previous collection efforts (Pool *et al.* 2012), and recorded male songs in 30 minute
349 intervals using 40-60 males per strain (raw individual recording measurements available
350 in Tables S3 and S4). Strains were assigned single trait values for each song behavior
351 representing the mean of individual replicates (Table S5).

352

353 In total, 37 traits were analyzed, many of which were found to have significant positive or
354 negative correlation, often between traits with *a priori* expectations of possible correlation
355 (e.g. the amount of song per minute and the number of bouts per minute are positively
356 correlated) (Figures 1, S1, S2). Among traits not correlated by definition, we noted the
357 strongest positive correlation between the sine and pulse amplitude traits, which could
358 suggest pleiotropy for song amplitude traits. Additionally, there was a strong negative
359 correlation between pulse carrier frequency and pulse mode preference, which could be
360 explained by a difference in amplitude between the two types of pulse song, which has
361 previously been demonstrated to correlate to carrier frequency (Clemens *et al*. 2018).

362 Interestingly, the FR and ZI cohorts of inbred song had slight variation in which traits were
363 correlated (Figure 1A).
364
365 Population mean trait values were compared statistically between France and Zambia
366 strain panels to test for significant trait divergence between populations in each examined
367 song characteristic (Figure 2; Table S5). Two related traits, described by Clemens *et al.*
368 (2020), had significant raw Mann-Whitney (MW) p-values for the population comparison:
369 the number of "fast" pulses ($p = 0.0185$) and fraction of "slow" pulses to total pulses ($p =$
370 0.0068; Figure 2A; Table S5). Hereafter, we focus on the latter of these correlated traits
371 (Figure 1AB) in light of its clearer signal of differentiation. Aside from these two
372 characteristics of pulse type, the only trait with even a marginal raw p-value ($p = 0.087$)
373 was the median amplitude of all pulses (Figure 2B; Table S5); France strains were
374 associated with somewhat higher (louder) pulse amplitudes than Zambia, on average.
375
376 We applied a permutation-based multiple test correction to MW p-values (Table S5).
377 Here, we found that the ratio of "slow" pulses to total pulses had the lowest least likelihood
378 of false positive discovery (~10%) and represented the greatest difference in population
379 trait differentiation (Figure 2; Table S5). Thus, the rate of slow to total pulses is likely to
380 represent a genuinely differentiated trait between the Zambia and France populations. In
381 contrast, there is weak evidence for population differentiation in pulse amplitude – which
382 showed little correlation with the slow/fast pulse traits (Figure S1). The pulse amplitude
383 difference was not significant after applying permutation-based multiple test correction
384 (indicating a 72% chance of getting at least one raw p-value as low as 0.088; Table S5).

385 Figure 2 demonstrates that both of these traits had somewhat overlapping interquartile
386 ranges, with more distinct distributions for pulse mode.
387
388 The above findings suggested that throughout the course of multiple courtship bouts in
389 an uninterrupted mating setting, males from France strains were relatively more likely to
390 utilize a fast pulse mode over a slow pulse mode. This trait's population differentiation
391 was also quantified by the Q_{ST} statistic, which yielded an elevated value of 0.797, which
392 exceeds the F_{ST} values of 96.44% of examined SNPs genome-wide (see Materials and
393 Methods). In general, Q_{ST} values that exceed the bulk of the genomic F_{ST} distribution are
394 often considered potential targets of geographically variable directional selection, and our
395 comparison conservatively used F_{ST} values from individual SNPs. Although this result
396 should also be interpreted in the context of the number of traits initially examined, it
397 suggests the possibility that the usage of fast versus slow pulses may have been
398 influenced by differential selection between populations, whether acting on this or a
399 pleiotropically correlated trait. Furthermore, the relatively consistent population
400 differentiation observed for this trait makes it an appropriate target for QTL analyses
401 involving phenotypically contrasting strains.
402
403 *SONG VARIATION BETWEEN RIL PARENTAL STRAINS REVEALS ADDITIONAL*
404 *TRAITS FOR MAPPING*
405 Next, we compared mean trait values between the two strains used in the establishment
406 of our RIL panel, FR320N and ZI418N ("parental" strains) (Figure 2 – dotted rectangles;
407 Table S5). Between these strains we found a total of 10 out of 37 traits with significant

raw MW p-values ($p<0.05$) (Table S5). The two song traits mentioned above with regard to population-level differences, pulse mode preference and median pulse amplitude, were represented among this set of traits (Figure 2A & 2B, dotted rectangles). The similarity in magnitude and direction of parental differences in these traits has important consequences for our ability to interpret mapping results as representing likely contributors to population differentiation, particularly for the pulse mode trait.

Seven additional traits displayed quantitatively significant differences between parental strains: the number of bouts per minute, the transition probability of 'null' (no) song to sine song, the median sine and pulse train length, median sine amplitude, and mode carrier frequencies of sines and pulses (Table S4). Quantitative differences in these traits between parental strains imply that mappable variation could exist in the RIL panel, and we therefore elected to map these traits in addition to the two previously mentioned. While mapping efforts for most of these traits will not reveal loci that contribute to significant population differentiation between populations, they could reveal loci that make a meaningful biological contribution to the production of courtship behavior.

SOME QTLS FOR TRAITS DIFFERENTIATED BETWEEN PARENTAL STRAINS INCLUDE KNOWN COURTSHIP GENES

We used a modified version of r/QTL (Broman *et al*. 2003; da Silva Ribeiro *et al.* 2024) to first map the song traits associated with parental strain but not population-level differences, under a single-locus QTL model. QTL mapping results for these traits are depicted in Figure 3 for the amount and type of song and in Figure 4 for the properties of

431 pulse or sine song, with full LOD profiles given in Table S6. For two traits, mode sine
432 carrier frequency and median sine amplitude, no genome-wide significant QTLs were
433 obtained. Conversely, a total of 21 significant QTL peaks were identified for the remaining
434 six traits, as described individually below (Table S7). Within each of these QTLs, we
435 highlight below any known genes associated with male mating behavior (Table S2).
436 However, not all QTLs include genes known to contribute to courtship behavior, and even
437 where they are present it is possible that other genes with currently unknown roles in
438 courtship behaviors may underlie some QTLs (Mackay 2009).
439
440 The average number of bouts per minute differed between the RIL parental strains (Table
441 S5) [FR320N (6.24+/-2.832) vs. ZI418N (7.831+/-2.294)] and mapped to two primary
442 QTLs on the X chromosome (Figure 3A; Table S7). The second interval (ChrX:10.6-11.4
443 Mb; note that all positions given here refer to *D. melanogaster* reference release 5.9) was
444 found to include two courtship genes from our annotated list, *discs large 1* (*dlg1*,
445 FBgn0001624) and *gustatory receptor 10b* (*Gr10b*, FBgn0030297).
446
447 Intuitively, a second parental-differentiated trait, the transition probability from null sound
448 to sine song was found to be correlated with the above-discussed bouts per minute trait.
449 As expected, this “Null to Sine” trait value was higher in the parental strain with greater
450 bouts per minute [ZI418N (0.005+/-0.004) vs. FR320N (0.003+/-0.002)] (Figure 2; Table
451 S5). In spite of the above-mentioned correlation with bouts per minute, the identified QTLs
452 for these traits were distinct, although some non-significant peaks coincided (Figure 3B).
453 The null to sine probability mapped to a region near the centromere on chromosome arm

454 2L starting at ~12.1 Mb (Figure 3B). This QTL's CI spans the low recombination
455 centromeric region and extends until chromosome arm 2R at ~7.04 Mb. Ten courtship-
456 associated genes were found in this interval, 4 of which encode gustatory receptors
457 (*Gr33a*, *Gr39a*, *Gr43a*, and *Gr47a*) (Table S8). Three genes that have been previously
458 established to play roles in male courtship initiation were also found in this interval (Table
459 S8). The gene *Chemosensory protein B 42a* (*CheB42a,* FBgn0053348) encodes a
460 pheromone-binding protein that plays a role in the rate and speed of courtship initiation
461 in males (Park *et al.* 2016). A neighboring gene, *pickpocket 25* (*ppk25*, FBgn0053349),
462 was similarly implicated in the initiation of courtship (Liu *et al.* 2012). Although the simplest
463 hypothesis would be that only a single gene is responsible for this QTL, the presence of
464 genes relevant to courtship initiation is notable with regard to the transition probability to
465 sine song.
466
467 The median lengths of sine and pulse trains were both significantly different between
468 parental strains, and shared positive correlations with one another (Figure 1A & 1B). In
469 both cases, train lengths were longer in the Zambian [sine: 0.094+/-0.032, pulse: 1.158+/-
470 0.136] cohort and shorter in the French cohort [sine: 0.078+/-0.025, pulse: 1.069+/-0.128]
471 (Figure 2; Table S5). Median pulse train length mapped to a single QTL with restrictive
472 peak Cis (Figure 3C; Table S7) between Chr2L:3.21-3.39 Mb that does not harbor
473 annotated male courtship-related genes. Whereas, we found that median sine train length
474 mapped to several separate QTLs on chromosome 3: three peaks on the left arm and two
475 peaks on the right arm (Figure 3D) (Table S7). A single QTL at Chr3R:12.1-12.6 Mb
476 overlaps a known courtship gene, *spineless* (*ss*, FBgn0003513) (Table S8).

477

478 We also investigated trait variation in the mode carrier frequency of pulse and sine songs,
479 which were higher in the France strain [211.7+/-40.7 versus 199.3+10.9 for pulses,
480 297.6+/-11.3 versus 291.9+/-5.5 for sines] (Figure 2; Table S5). Pulse carrier frequency
481 mapped to a single primary QTL on chromosome 3L (Figure 4A & 4B; Table S7) and was
482 not found to harbor known courtship genes. There was no significant QTL associated with
483 sine carrier frequency, and underlying LOD landscapes suggest that, as with train lengths,
484 sine and pulse carrier frequencies may be governed by unique loci (Figure 4A & 4B, Table
485 S7). This trend is somewhat recapitulated in mapping the amplitude of pulse (Figure 4C)
486 and sine song (Figure 4D), although no QTLs were detected for the latter trait.

487

488 Relative to the above traits, the median amplitude of pulses gave a relatively more
489 polygenic signal, mapping to 11 unique QTLs that form roughly three clusters across
490 chromosome 3 (Figure 4C; Table S7). The two most statistically significant peaks mapped
491 to chromosome 3L (inclusive Cis 3L:5.98-6.71 Mb and 3L:6.80-7.24 Mb) and were flanked
492 by two 'minor' peaks (Figure 4A; Figure S5; Figure S6; Table S7). The more significant of
493 these two (peak 3) contains the courtship-associated gene *pale* (*ple,* FBgn0005626). *Pale*
494 encodes a rate-limiting enzyme involved in catecholamine synthesis, such as the
495 production of dopamine precursors, and has been demonstrated to play roles in a variety
496 of behaviors, including courtship (Liu *et al.* 2009).

497

498 A second cluster on chromosome 3L harbored 5 additional QTLs, ranging between 3L:11
499 Mb and 3L:16.5 Mb and spaced roughly 1 Mb apart (Figure 4C). Peak 5 (Figure S6, Table

500 S8) contains a second identified courtship-associated gene, the gustatory receptor *Gr68a*
501 (FBgn0041231). The third cluster on chromosome 3R contained the final two QTLs, which
502 each have confidence intervals within the 3R:10.5-13.4 Mb region. Because this trait
503 showed possible evidence of population differentiation, for completeness we report a
504 scan for local adaptation statistic outliers (Materials and Methods; Figures S5 & S6; Table
505 S8; Table S9). However, we emphasize that the evolutionary forces underlying variation
506 in this trait remain uncertain.
507
508 *COMPOSITE TRAIT ANALYSIS YIELDS UNIQUE QTL LANDSCAPES OF TWO SONG*
509 *TRAITS*
510
511 The extent of correlation among song traits (Figure 1) and occasional similarity in LOD
512 landscapes of QTL maps suggested that some overlapping QTLs between traits could
513 reflect pleiotropy. While full multivariate trait mapping departs from the focus of the
514 present study on connections between genomic regions and specific aspects of song, we
515 did investigate the potential for pleiotropy contributing to overlapping QTLs by performing
516 residual trait mapping between specific pairs of traits. In general, for two traits with higher
517 and lower LD scores involving their overlapping QTL peaks, we obtained residuals for the
518 lower-LOD trait after performing a linear regression of its trait values against the higher-
519 LOD trait. These residuals, which reflect the RIL variation in the lower trait not explained
520 by its correlation with the higher trait, were then used in our standard QTL mapping
521 pipeline.
522

523 One pair of positively correlated traits – median sine train length and median pulse
524 amplitude (Figure 1) – had two overlapping peaks. Between these two pairs of
525 overlapping QTLs, each trait had the higher LOD score in one case (Figure S2A; Figure
526 S3; Table S10), and therefore regression and residual mapping were performed in both
527 directions. When the residual trait values for median pulse amplitude were mapped, six
528 chromosome 3 QTLs remained, one of which overlapped the original peak of interest,
529 while another contained the courtship-associated gene *doublesex* (Table S9). When the
530 residual trait values of median sine train length were mapped instead, all five of that trait's
531 originally significant chromosome 3 QTLs were eliminated, but a novel QTL peak on the
532 X chromosome was detected [C.I. approx. X:4.14Mb-4.41Mb], which did not harbor any
533 known annotated courtship genes (Figure S3A). Hence, among the two intially
534 overlapping peaks, there is evidence for a locus underlying pulse amplitude that can not
535 be explained by that trait's overlap with sine train length, whereas the QTL signal
536 observed for sine train length could be explained via pleiotropy with pulse amplitude.
537
538 Another instance of QTL peak overlap occurred between the pulse carrier frequency and
539 median pulse amplitude traits, which shared an overlap within the pulse carrier frequency
540 single significant peak (Figure 4A, 4C; Table S7). When fit to median pulse amplitude, the
541 residual trait values of pulse carrier frequency did not yield significant QTL (Figure S3C).
542 This result may imply that the QTL signal for pulse carrier frequency is driven primarily by
543 its pleiotropic relationship with median pulse amplitude. Our results are consistent with
544 previous evidence of a positive relationship between these traits (Clemens *et al*. 2018),

545 and that males with silenced motoneurons produce pulse song that is decreased in both
546 amplitude and carrier frequency (Shirangi *et al*. 2014).
547
548 Lastly, we performed a linear regression between median sine amplitude and median
549 pulse amplitude song traits (Figure S4). These traits displayed the strongest positive
550 correlations in both inbred and RIL datasets (Figures 1, S1, S2). These traits did not share
551 overlapping QTLs (initial mapping of median sine amplitude did not reveal any significant
552 QTL). However, they did share very similar overall QTL landscapes, and a nearly-
553 significant QTL for sine amplitude aligned closely with the strongest QTL for pulse
554 amplitude (Figures 4C and 4D). Residual mapping revealed a novel QTL for median sine
555 amplitude on chromosome 3R [C.I. approx. 3R:19.35Mb-19.98Mb], which does not harbor
556 known annotated courtship genes. (Figure S4). When comparing the initial sine amplitude
557 QTL landscape to the residual trait landscape, we found that many of the non-significant
558 peak signals on chromosome 3L were “flattened” or had diminished signal in the residual
559 map, consistent with much of the trait signal on chromosome 3L being driven by one or
560 more genetic factors underlying the correlation of these two amplitude traits.
561
562 *A SONG TRAIT DIFFERENTIATED BETWEEN FRANCE AND ZAMBIA POPULATIONS*
563 *YIELDS A SINGLE STRONG QTL*
564 We next mapped the song trait that represented the most geographically differentiated
565 trait among those studied (Figure 2; Table S5). The ratio of slow pulses to the total number
566 of pulses, which was significantly higher in the Zambian strains relative to France strains
567 (0.833+/-0.067 vs. 0.725+/-0.125, respectively) (Figure 2A; Table S5). One major QTL

568 peak on chromosome 3R was identified with a broad CI interval at approximately
569 3R:20.0..22.6 Mb (Figure 5A; Table S7), which was estimated to explain 42% of the
570 parental strain trait difference.
571
572 This trait was estimated to have approximately a 90% probability of reflecting genuine
573 population differentiation, and presented a Q_{ST} value consistent with the differential action
574 of directional selection (on either this or a pleiotropically correlated trait) between
575 populations. Under the hypothesis that a gene underlying a trait with elevated population
576 differentiation might display elevated genetic differentiation, we chose to supplement our
577 QTL mapping with a population genetic analysis of the detected QTL region, in which we
578 identified genomic windows within the QTL's restrictive CIs that were associated with
579 values of either window F_{ST}, maximum SNP F_{ST} (da Silva Ribeiro *et al.* 2022) or the
580 Comparative Haplotype Identity statistic (Lange & Pool 2016) within the top 1% on the
581 chromosome arm (Materials and Methods; Table S9). We also made note of an expanded
582 range of candidate genes on functional grounds, including nervous system genes and
583 those related to wing development.
584
585 The highest LOD scores within this QTL were amongst a group of restrictive CI regions
586 (*i.e.* intervals within 1.5 LODs of the QTL maximum) toward the distal/right side of this
587 QTL. Within one of these restrictive CI regions, we identified a cluster of outlier statistics
588 around 3R:21.75-22 Mb (Figure 5B, orange intervals; Materials and Methods; Table S7).
589 Within this gene-dense region is the *enhancer of split* complex and flanking genes, which
590 have been previously implicated in the quantitative trait mapping of courtship behavior

591 (Moehring & Mackay 2004). Additionally, the transcriptional corepressor *groucho* (*gro*,
592 FBgn0001139) falls within this region (Figure 5B), and has been implicated in the
593 *retained*-mediated repression of transcriptional targets involved in male courtship
594 behavior (Shirangi *et al.* 2006).
595
596 Two additional male courtship genes were found within other restrictive CI regions of this
597 same QTL (Figure 5B; Table S8). Near the middle of the full QTL region, the gene *takeout*,
598 a lipid binding protein that is a target of the sex determination pathway and implicated in
599 male courtship (Dauwalder *et al.* 2002), is flanked by highly differentiated windows (Figure
600 5B). Toward the proximal/left side of the QTL, the *slowpoke* gene, which has a
601 demonstrated role in sine song carrier frequency variation in the *D. simulans* clade (Ding
602 *et al.* 2016) is present within the restrictive CI. This gene does not overlap or adjoin any
603 population genetic outlier windows (Figure 5B), but this pattern does not exclude the
604 possibilities of elevated differentiation at more distant regulatory regions or a causative
605 locus that lacks a strong population genetic signal.
606
607 Three additional regions of this QTL's restrictive CIs were found to contain population
608 genetic outlier windows (Figure 5; Table S9). The first window contains the gene *jaguar*
609 (*jar*, FBgn0011225). The second window overlaps three genes: *BRWD3*, *Rrp5*, and *Dis3*
610 (FBgn0011785, FBgn0039182, FBgn00339183). The third window does not contain any
611 genes, but sits upstream of the first exon of the closest proximal gene, *Furin-1* (*Fur1,*
612 FBgn0004509). This gene has known roles in synaptic transmission at neuromuscular
613 junctions (Kim *et al.* 2015), and its disruption via RNA-interference is associated with

614 abnormal locomotion and flight (Schnorrer *et al.* 2010). Although we highlight multiple
615 potential genes that may underlie this QTL, we note that it may be driven by any one of
616 them, by more than one of them, or by none of those listed above.

617 DISCUSSION

618 Here we describe natural variation in male courtship song components between two
619 natural populations of *D. melanogaster* from contrasting environments. Comparison of
620 population cohorts revealed significant phenotypic differences in pulse mode preference,
621 and relatedly the total number of fast pulses performed in the assay. We found that the
622 slow to fast preference is partially explained by a QTL with moderate effect size.
623 Conversely, the median amplitude of pulses, which had limited support for population
624 differentiation, was found to be under the control of multiple QTL intervals of relatively
625 small effects. Other traits differentiated between the RIL parental strains had anywhere
626 from zero to six significant QTLs detected. However, in light of the total effect sizes
627 estimated across QTLs for each trait (Table S7), along with the finite statistical power
628 expected for detecting QTLs from a few hundred RILs (*e.g.* King *et al.* 2012), we would
629 predict that each of these traits is also influenced by an unknown number of smaller effect
630 loci that did not achieve genome-wide significance in our mapping study.

631

632 *Phenotypic variability among RIL parental strains reveals unique QTL for multiple*
633 *courtship traits*

634 Mapped traits that did not have significant differences at the population level but did
635 display significant parental strain differences were mapped in an attempt to identify genes
636 that may regulate courtship behavior. Components of courtship behavior are responsive

637 to artificial selection in lab settings using wild-derived populations (Ritchie & Kyriacou
638 1994; Gaertner *et al*. 2015), reinforcing the view that fitness-relevant variation in courtship
639 behaviors may be present within natural populations. The generation of a RIL panel from
640 two inbred strains will capture a limited quantity of naturally segregating variation, but the
641 origins of our parental strain from two distinct natural populations may have enhanced the
642 extent of trait variation in behavior that is amenable to QTL mapping.
643
644 Aside from pulse mode preference, we found that four of eight parental-differentiated
645 traits yielded significant QTLs overlapping known courtship-related genes (Table S2;
646 Table S8), and our results provide a preliminary association of these male song
647 components with previously implicated genes. Most of the significant QTL were found on
648 autosomes (Figures 3 & 4), with only two neighboring QTLs for the same trait identified
649 on the X chromosome. (Y chromosome effects were not considered in the present study,
650 due to the absence of available RIL sequencing data from males) While the total number
651 of QTLs and the linkage that exists among some of them preclude strong conclusions
652 regarding X-linkage, a reduced occurrence of X-linked QTLs might be predicted if genes
653 involved in male song production are sometimes subject to sexually antagonistic selective
654 pressures (Snook *et al.* 2005), in light of the X chromosome spending two thirds of its
655 time in females.
656
657 In general, we found that even when corresponding pulse and sine song traits both
658 differed between RIL parental strains, they mapped to distinct genomic intervals. This
659 pattern held for pulse versus sine train length (Figure 3C & 3D; Table S7) and for pulse

660 versus sine carrier frequency (Figure 4A & 4B; Table S7), in agreement with the lack of
661 strong correlations between these traits (Figure S1). This evidence for distinct genetic
662 architectures, in spite of co-directional differences in these pulse and sine song traits
663 between our France and Zambia parental strains, supports previous findings that
664 components of sine and pulse song can have unique genetic (and neuronal) bases
665 (Shirangi *et al.* 2013; Ding *et al.* 2016; Hiroshi *et al.* 2022; Shiozaki *et al.* 2023; Lillvis *et*
666 *al.* 2024). In contrast, we found that the nearly genome-wide significant (p = 0.06) peak
667 for sine amplitude (Figure 4D) falls within the inclusive CI of the most significant QTL for
668 pulse amplitude, at roughly 3L:6.30 Mb – 6.32 Mb (Figure 4C; Table S7, peak 3). The
669 potentially overlapping architecture of the two amplitude traits may indicate a pleiotropic
670 basis and aligns with the stronger correlation between these traits within both populations
671 (Figure S5, S6).
672
673 *The rate of slow to fast pulses is the most phenotypically differentiated song trait between*
674 *Zambia and France populations and involves a single detectable QTL*
675 Among the 37 song traits examined here, two traits related to pulse mode usage,
676 particularly the preference for slow versus fast pulses, received the strongest statistical
677 support for differentiation between the France and Zambia populations examined. The
678 distinction between fast and slow pulse modes is a relatively recent discovery and its
679 possible role in sexual selection is currently unknown, although the trait does seem to
680 affect female movement responses to song (Clemens *et al.* 2018). This same study
681 showed that males use sensory input (primarily visual) to bias which pulse mode is used
682 (Clemens *et al.* 2018).

683

684 Assay conditions, such as chamber size and female behavioral plasticity are thus an
685 important consideration when interpreting results regarding this trait. Recording
686 chambers used in the study were small (Arthur *et al.* 2013), constraining flies to a minimal
687 space. We did not track the positions of flies during courtship, so we cannot rule out that
688 male song varied in response to female signals. The difference in pulse mode preference
689 in the present study may either represent a cumulative difference in male response to
690 females, or simply represent a difference in a probabilistic preference of pulse choice
691 when other environmental parameters are held constant. Still, QTL signals for this trait
692 were very strong (Figure 5A) and suggest that population genetic differentiation underlies
693 trait differences.

694

695 Our analysis provides evidence that pulse usage may have been influenced either directly
696 or indirectly by population-specific directional selection. In a conservatively designed
697 comparison between Q_{ST} and F_{ST}, the pulse type ratio showed greater differentiation than
698 all but around 3.5% of genome-wide SNPs. If pulse type usage has in fact been influenced
699 by recent directional selection, the reasons remain unclear. Although female preference
700 varies between some southern African and European strains, there is no documented
701 role of courtship song in M/Z-type mating preference (Colegrave *et al.* 1999). Hence, it is
702 unclear to what degree any directional selection has resulted in song differentiation that
703 impacts male reproductive fitness. However, it is worth emphasizing that all experiments
704 in this study were conducted at room temperature. In contrast, the far more variable
705 temperatures encountered by natural populations, especially in the temperate zone, may

exert plastic influences on song components (Stanley & Kyriacou 2021), and it is possible that genetic adaptation may allow for the production of universally favorable song characteristics across divergent environments, even if some specific song differences persist at a given temperature.

Alternatively, it is possible that directional selection, if present here, may not have been acting upon song at all. Population genomic scans for selection in this species have reported evidence for local adaptation between warm- and cold-adapted natural populations for multiple categories of genes that modulate synaptic function, including neuropeptide receptors, ion channels, and structural components of the synapse (*e.g.* Pool *et al.* 2017). It is possible that the adaptive evolution of one or more aspects of synaptic function, even if driven by selection to maintain nervous system function in a novel environment, might have pleiotropic consequences for behaviors such as those involved in courtship song. Adaptive responses to other selective pressures, such as insecticides, some of which target insect nervous systems, also may trigger pleiotropic effects on traits that are not the direct target of selection. Hence, further study will be needed to assess whether pulse mode usage has been targeted or pleiotropically influenced by directional selection between African and European *D. melanogaster* populations.

The pleiotropy hypothesis could potentially also explain variation in amplitude (*i.e.* volume), which showed weaker evidence of differentiation between populations. Pulse amplitude was found to be somewhat higher in France than Zambia males (Figure 2;

729 Table S5), sine amplitude showed a lesser trend in the same direction, and both traits
730 were significantly higher in the France parental strain than in the Zambia parent (Table
731 S5). Flies from these populations tend to be slightly larger (Lack *et al.* 2016b). Based on
732 measurements of females from that study, the France RIL parent has 8.1% greater thorax
733 length and 5.5% greater wing width than the Zambia RIL parent. If larger flies tend to sing
734 with greater volume, then differences in amplitude could be downstream of differences in
735 body or wing size. Empirically, this relationship is unclear, although there is indirect
736 evidence that physical size of wing components, such as the musculature, can play roles
737 in the sexually dimorphic expression of male song (Shirangi *et al.* 2013). Further research
738 will be needed to determine the degree to which song variation and differentiation within
739 *D. melanogaster* is shaped by directional selection to modify or maintain sexually-
740 selected traits in populations experiencing different environments, directional selection on
741 pleiotropically correlated traits, stabilizing selection, genetic drift, or other forces.
742
743 We identified a single large-effect QTL for pulse mode usage on chromosome arm 3R.
744 Curiously, this QTL for the trait with the strongest evidence for population differentiation
745 had a stronger mapping signal than any of the 21 QTLs identified for any of the other
746 traits that differed between the RIL parent strains. This QTL had a somewhat bimodal
747 shape (Figure 5A) that could reflect either stochastic factors in QTL mapping or else the
748 contribution of more than one locus.
749
750 In *Drosophila*, an average QTL may encompass hundreds of genes (Mackay 2001).
751 Functional approaches, such as complementation tests or gene disruption experiments,

752 have traditionally been employed to identify candidate genes from QTL intervals, but can
753 become a laborious task when attempting to test all possible candidates within a QTL CI.
754 We thus supplemented our QTL mapping with a population genetic analysis of QTL
755 intervals, leveraging available population genomic data (Lack *et al.* 2016a) to identify
756 specific loci with elevated genetic differentiation between populations that might
757 contribute to elevated trait differentiation. The candidates identified for pulse model
758 preference, such as the region surrounding the *enhancer of split* complex, *groucho*,
759 *takeout*, and other genes (Figure 5B; Table S8), provide promising candidates to be
760 tested in future studies. Subsequent analyses such as fine mapping and functional testing
761 such as via reciprocal hemizygosity tests (Stern 2014) may ultimately confirm specific
762 genes that contribute to population differences in courtship song.
763
764 Collectively, our results provide evidence of variation in pulse song usage between
765 naturally occurring populations of *D. melanogaster*. By combining RIL-based QTL
766 mapping with population genetic inference, we identified a set of genes that may be tested
767 in future studies. We also note that all 37 traits examined showed meaningful variation
768 among the studied strains, further reinforcing the vast potential of natural variation for
769 investigating the genetic mechanisms underlying behavior.
770

771 ACKNOWLEDGMENTS

772 We thank Ben Arthur and Joshua Lillvis for assistance with song analysis and members
773 of the Pool Lab for helpful comments on this manuscript. This work was funded by NIH

774 grant R35 GM13630 to J.E.P. and by the HHMI Janelia Research Campus Visitor Project
775 Program.

776

777 DATA AVAILABILITY STATEMENT

778 All raw trait data is provided in this article's Supplemental Tables. No new genomic
779 sequencing data was generated for this study. RIL sequence data reported by da Silva
780 Ribeiro *et al.* (2024) is available from the NIH Sequence Read Archive (BioProject:
781 PRJNA861300).

782

783 CONFLICT OF INTEREST

784 The authors declare that they have no conflicts of interest.

785 CITATIONS

786

787 Anholt RRH, O'Grady P, Wolfner MF, Harbison ST. 2020. Evolution of Reproductive
788 Behavior. *Genetics*. 214:49-73.

789

790 Arbuthnott D. 2009. The genetic architecture of insect courtship behavior and premating
791 isolation. *Heredity.* 103:15-22.

792

793 Arthur BJ, Sunayama-Morita T, Coen P, Murthy M, Stern DL. 2013. Muli-channel acoustic
794 recording and automated analysis of *Drosophila* courtship songs. *BMC Biol*. 11:11.

795

796 Arthur BJ, Ding Y, Sosale M, Khalif F, Kim E, Waddell P, Turaga SC, Stern DL. 2021.
797 Songexplorer: a deep learning workflow for discovery and segmentation of animal
798 acoustic communication signals. *bioRxiv*. 2021-03.

799

800 Begun DJ, Aquadro, CF. 1993. African and North American populations of *Drosophila*
801 *melanogaster* are very different at the DNA level. *Nature*, 365:548–550.

802

803 Bennet-Clark HC, Ewing AW. 1969. Pulse interval as a critical parameter in the courtship
804 song of *Drosophila melanogaster. Anim Behav*. 17:755-759.

805

806 Broman KW, Wu H, Sen Ś, Churchill GA. 2003. R/qtl: QTL mapping in experimental
807 crosses. *Bioinformatics.* 19:889-890.

Clemens J, Coen P, Remschied FA, Pereira TD, Mazumder D, Aldarondo DE, Pacheco DA, Murthy M. 2018. Discovery of a New Song Mode in *Drosophila* Reveals Hidden Structure in the Sensory and Neural Drivers of Behavior. *Curr Biol.* 28:2400-2412.

Colegrave, Hollocher, Hinton, Ritchie. 1999. The courtship song of African *Drosophila melanogaster. J Evol Biol*. 13:143-150.

Cook RM. 1973. Courtship processing in *Drosophila melanogaster*. II. An adaptation to selection for receptivity to wingless males. *Anim Behav*. 21:349-358.

Corbett-Detig R & Nielsen R. 2017. A Hidden Markov Model Approach for Simultaneously Estimating Local Ancestry and Admixture Time Using Next Generation Sequence Data in Samples of Arbitrary Ploidy. PLOS Genet. 13(1): e1006529.

Cowling DE, Burnet B. 1981. Courtship songs and genetic control of their acoustic characteristics in sibling species of the *Drosophila melanogaster subgroup. Anim Behav.* 29:924-935

da Silva Ribeiro T, Galván JA, Pool JE. 2023. Maximum SNP F_{ST} Outperforms Full-Window Statistics for Detecting Soft Sweeps in Local Adaptation. *Genome Biol Evol*. 7:evac143.

da Silva Ribeiro T, Lollar MJ, Sprengelmeyer QD, Huang Y, Benson DM, Orr MS, Johnson ZC, Corbett-Detig RB, Pool JE. Recombinant inbred line panels inform the genetic architecture and interactions of adaptive traits in *Drosophila melanogaster*. *bioRxiv* 2024-05.

Dauwalder B, Tsujimoto S, Moss J, Mattox W. 2002. The *Drosophila takeout* gene is regulated by the somatic sex-determination pathway and affects male courtship behavior. *Genes Dev*. 16:2879-2892

David JR, Capy P. 1988. Genetic variation of *Drosophila melanogaster* natural populations. *Trends in Genetics*. 4:106–111.

Ding Y, Berrocal A, Morita T, Longdon KD, Stern DL. 2016. Natural courtship song variation caused by an intronic retroelement in an ion channel gene. *Nature.* 536:329-332.

Ding Y, Lillvis JL, Cande J, Berman GJ, Arthur BJ, Long X, Xu M, Dickson BJ, Stern DL. 2019. Neural Evolution of Context-Dependent Fly Song. *Curr Biol.* 29:1089-1099.

Drosophila 12 Genomes Consortium; Clark AG, Eisen MB, Smith DR, *et. al.* 2007. Evolution of genes and genomes on the Drosophila phylogeny. *Nature*. 450: 203-218.

Dukas R. 2005. Learning affects mate choice in female fruit flies. *Behavioral Ecology*. 16(4):800-804.

Ewing AW, Bennet-Clark HC. 1968. The courtship songs of *Drosophila. Behaviour*. 31:288-301.

Fabian DK, Lack JB, Vinayak M, Schlötterer C, Schmidt PS, Pool JE, Flatt, T. 2015. Spatially varying selection shapes life history clines among populations of *Drosophila melanogaster* from sub-Saharan Africa. *J Evol Biol*. 28:826–840.

Fitzgerald TD, Peterson SC. 1988. Cooperative Foraging and Communication in Caterpillars. *Bioscience.* 38:20-25.

Gaertner BE, Ruedi EA, McCoy LJ, Moore JM, Wolfner MF, Mackay TFC. Heritable variation in courtship patterns in *Drosophila*. *G3*. 5:531-539.

Gavrilets S, Vose A. 2007. Case studies and mathematical models of ecological speciation. 2. Palms on an oceanic island. *Mol. Ecol.* 16:2910-2921.

Gleason JM, Nuzhdin SV, Ritchie MG. 2002. Quantitative trait loci affecting a courtship signal in *Drosophila melanogaster*. *Heredity.* 89:1-6.

875 Gleason JM. 2005. Mutations and Natural Genetic Variation in the Courtship Song of
876 *Drosophila. Behav Genet.* 35:265-277.
877
878 Greenfield MD. 2016. Evolution of Acoustic Communication in Insects. *Insect Hearing*.
879 Springer. Manhattan (NY).
880
881 Greenspan, RJ, Ferveur, JF. 2000. Courtship in Drosophila. *Annu Rev Genet.* 34:205-
882 232.
883
884 Grillet M, Everaerts C, Houot B, Ritchie MG, Cobb M, Ferveur JF. 2012. Incipient
885 speciation in *Drosophila melanogaster* involves chemical signals. *Sci Rep.* 2:224.
886
887 Hollocher H, Wu C-I. 1996. The genetics of reproductive isolation in the *Drosophila*
888 *simulans* clade: X vs. autosomal effects and male vs. female effects. *Genetics.* 143:1243-
889 1255.
890
891 Hope KA, Flatten D, Cavitch P, May B, Sutcliffe JS, O'Donnell J, Reiter LT. 2019. The
892 Drosophila Gene *Sulfateless* Modulates Autism-Like Behaviors. *Front Genet.* 10:574.
893
894 Iglesias PP, Hasson E. 2017. The role of courtship song in female mate choice in South
895 American Cactophilic *Drosophila. PLoS ONE.* 12:e0176119.
896

Keller A. 2007. *Drosophila melanogaster*'s history as a human commensal. *Curr Biol*. 17:R77-R81.

Keller L, Surette MG. 2006. Communication in bacteria: an ecological and evolutionary perspective. *Nat Rev Microbiol.* 4:249-58.

Kim YJ, Igiesuorobo O, Ramos CI, Bao H, Zhang B, Serpe M. 2015. Prodomain removal enables Neto to stabilize glutamate receptors at the *Drosophila* neuromuscular junction. *PLoS Genet*. 11:e1004988

King EG, Merkes CM, McNeil CL, Hoofer SR, Sen S, Broman KW, Long AD, Macdonald SJ. 2012. Genetic dissection of a model complex trait using the *Drosophila* Synthetic Population Resource. *Genome Res*. 22:1558-1566.

Lachaise D, Carious ML, David JR, Lemeunier F, Tsacas L, Ashburner M. 1988. Historical biogeography of the *Drosophila melanogaster* species subgroup. *Evol Biol*. 22:159-225.

Lachaise D, Silvain JF. 2004. How two Afrotropical endemics made two cosmopolitan human commensals: the *Drosophila melanogaster-D. simulans* palaeogeographic riddle. *Genetica.* 120:17-39.

Lack JB, Lange JD, Tang AD, Corbett-Detig RB, Pool JE. 2016a. A thousand fly genomes: an expanded *Drosophila* Genome Nexus. *Mol Biol Evol*. 33:3308-3313.

Lack JB, Monette MJ, Johanning EJ, Sprengelmeyer QD, Pool JE. 2016b. Decanalization of wing development accompanied the evolution of large wings in high altitude *Drosophila*. *Proc Natl Acad Sci USA*. 113: 1014–1019.

Lande R. 1992. Neutral theory of quantitative genetic variance in an island model with local extinction and recolonization. *Evolution*. 46:381-389

Lange JD, Pool JE. 2016. A haplotype method detects diverse scenarios of local adaptation from genomic sequence variation. *Mol Ecol.* 25:3081-3100

Laturney M, Moehring AJ. 2012. The Genetic Basis of Female Mate Preference and Species Isolation in *Drosophila. Intl J Evol Biol.* 2012:328392

Leonhardt SD, Menzel F, Nehring V. 2016. Ecology and Evolution of Communication in Social Insects. *Cell.* 164:1277-1287.

Lieberman P. 1971. On the Evolution of Human Language. *Speech Res.* 113-131.

Lillvis JL, Wang K, Shiozaki HM, Stern DL, Dickson BJ. Nested neural circuits generate distinct signals during *Drosophila* courtship. *Curr Biol*. 34:808-824.

942 Liu T, Dartevelle L, Yuan C, Wei H, Wang Y, Ferveur JF, Guo A. 2009. Reduction of
943 dopamine level enhances the attractiveness of male *Drosophila* to other males. *PLoS*
944 *ONE*. 4:e4574.
945
946 Liu T, Starostina E, Vijayan V, Pikielny CW. 2012. Two *Drosophila* DEG/ENaC Channel
947 Subunits Have Distinct Functions in Gustatory Neurons That Activate Male Courtship. *J*
948 *Neurosci.* 32:11879-11889.
949
950 Mackay TFC. 2001. The Genetic Architecture of Quantitative Traits. *Annu Rev Genet.*
951 35:303-339.
952
953 Mackay TFC, Heinsohn SL, Lyman RF, Moehring AJ, Morgan TJ, Rollmann SM. 2005.
954 Genetics and genomics of *Drosophila* mating behavior. *Proc Natl Acad Sci USA*.
955 102:6622-6629.
956
957 Mackay TFC. 2009. The genetic architecture of complex behaviors: lessons from
958 *Drosophila. Genetica.* 136:295-302.
959
960 Manning A. 1967. The control of sexual receptivity in female *Drosophila. Anim Behav.*
961 15:239-250.
962
963 Maynard Smith J. 1979. Game theory and the evolution of behaviour. *Proc R Soc Lond*
964 *B.* 205:475-488.

Moehring AJ, Mackay TFC. 2004. The quantitative genetic basis of male mating behavior in *Drosophila melanogaster.* Genetics. 167:1249-1263.

O'Grady P, DeSalle R. 2018. Phylogeny of the Genus *Drosophila*. *Genetics.* 209:1-25.

Oh KP, Fergus DJ, Grace JL, Shaw KL. 2012. Interspecific genetics of speciation phenotypes: song and preference coevolution in Hawaiian crickets. *J Evol Biol.* 25:1500-1512.

Park SK, Mann KJ, Lin H, Starostina E, Kolski-Andreaco A. 2006. A *Drosophila* protein specific to pheromone-sensing gustatory hairs delays males' copulation attempts. *Curr Biol.* 16:P1154-1159,

Pool JE, Aquadro CF. 2007. The genetics basis of adaptive pigmentation variation in *Drosophila melanogaster. Mol Ecol.* 16:2844-2851.

Pool JE, Corbett-Detig RB, Sugino RP, Stevens KA, Cardeno CM, Crepeau MW, Duchen P, Emerson JJ, Saelao P, Begun, DJ, Langley CH. 2012. Population genomics of sub-Saharan *Drosophila melanogaster*: African diversity and non-African admixture. *PLoS Genet*. 8:e1003080.

Pool JE, Braun DT, Lack JB. 2017. Parallel evolution of cold tolerance within *Drosophila melanogaster. Mol Biol Evol*. 34:349-360.

Price TD. 2002. Domesticated birds as a model for the genetics of speciation by sexual selection. *Genetica*. 116:311-327.

Prum RO. 1990. Phylogenetic analysis of the evolution of display behavior in the Neotropical manakins (Aves, Pipridae). *Ethology*. 84:202-231.

R Core Team. 2023. R: A Language and Environment for Statistical Computing. R Foundation for Statistical Computing, Vienna, Austria. <https://www.R-project.org/>

Riabinina O, Dai M, Duke T, Albert JT. 2011. Active Process Mediates Species-Specific Tuning of Drosophila Ears. *Curr Biol.* 21:658-664.

Ritchie MG, Yate VH, Kyriacou CP. 1994. Genetic variability of the interpulse interval of courtship song among some European populations of *Drosophila melanogaster*. *Heredity.* 72:459-464.

Ritchie MG, Halsey EJ, Gleason JM. 1999. *Drosophila* song as a species-specific mating signal and the behavioural importance of Kyriacou & Hall cycles in *D. melanogaster* song. *Anim Behav.* 58:649-657.

1010 Rockman MV. 2012. The QTN program and the alleles that matter for evolution: All that's
1011 gold does not glitter. *Evolution*. 66:1-17.
1012
1013 Schnorrer F, Schönbauer C, Langer CHC, Dietzl G, Novatchkova M, Schernhuber M,
1014 Fellner M, Azaryan A, Radolf M, Stark A, Keleman K, Dickson BJ. 2010. Systematic
1015 genetic analysis of muscle morphogenesis and function in *Drosophila*. *Nature*. 464:287-
1016 291.
1017
1018 Shahandeh MP, Turner TL. 2020. The complex architecture of male mate choice
1019 evolution between *Drosophila* species. *Heredity.* 124:737-750.
1020
1021 Shirangi TR, Taylor BJ, McKeown M. 2006. A double-switch system regulates male
1022 courtship behavior in male and female Drosophila melanogaster. *Nat Genet*. 38:1435-
1023 1439.
1024
1025 Shirangi TR, Stern DL, Truman JW. 2013. Motor control of *Drosophila* courtship song.
1026 *Cell Rep*. 5:678-86.
1027
1028 Shiozaki HM, Wang K, Lillvis JL, Xu M, Dickson BJ, Stern DL. 2023. Combinatorial
1029 dynamics orchestrate flexible motor patterns in *Drosophila* courtship. *bioRxiv*.
1030 doi:10.1101/2022.12.14.520499.
1031

1032 Sinclair CS, Lisa SF, Pischedda A. 2021. Does sexual experience affect the strength of
1033 male mate choice for high-quality females in *Drosophila melanogaster*? *Ecology and*
1034 *Evolution*. 11:16981-16992. Doi:10.1002/ece3.8334.
1035
1036 Snook RR, Robertson A, Crudgington HS, Ritchie MG. 2005. Experimental manipulation
1037 of sexual selection and the evolution of courtship song in *Drosophila pseudoobscura*.
1038 *Behav Genet*. 35:245-255.
1039
1040 Speith H. 1952. Mating behavior within the genus *Drosophila* (Diptera). *Bull Am Mus Nat*
1041 *Hist*. 99:399-474.
1042
1043 Spitze K. 1993. Population structure in *Daphnia obtusa*: Quantitative genetic and
1044 allozyme variation. *Genetics*. 135:67-374.
1045
1046 Sprengelmeyer QD, Mansourian S, Lange JD, Matute DR, Cooper, BS, Jirle, EV,
1047 Stensmyr MC, Pool JE. 2020. Recurrent collection of *Drosophila melanogaster* from wild
1048 African environments and genomic insights into species history. *Mol Biol Evol*. 11:15354-
1049 15376.
1050
1051 St. Johnston D. 2002. The art and design of genetic screens: Drosophila melanogaster.
1052 *Nat Rev Genet.* 3:176-188
1053

Strömnæs Ö, Kvelland I. 1962. Sexual activity of *Drosophila melanogaster* males. *Hereditas. 48(3):442-470.*

Stanley RA, Kyriacou CP. 2021. A latitudinal cline in a courtship song character of *Drosophila melanogaster. J Neurogenet.* 35:333-340

Stern DL. 2014. Reported *Drosophila* courtship song rhythms are artifacts of data analysis. *BMC Biol.* 12:38.

Sturtevant AH 1915. Experiments on sex recognition and the problem of sexual selection in Drosophila. *J Anim Behav*. 5:351-366.

Swain B, von Philipsborn AC. 2021. Chapter Three - Sound production in *Drosophila melanogaster*: Behavior and neurobiology. Amsterdam (Netherlands): Elsevier.

Talyn BC, Dowse HB. 2004. The role of courtship song in sexual selection and species recognition by female *Drosophila melanogaster. Anim Behav.* 68:1165-1180

The MathWorks Inc. 2022. MATLAB version: 9.13.0 (R2022b), Natick, Massachusetts: The MathWorks Inc. <https://www.mathworks.com>

Turissini, DA, Mcgirr, JA, Patel, SS, David, JR, Matute, DR. 2018. The Rate of Evolution of Postmating-Prezygotic Reproductive Isolation in *Drosophila. Mol Biol Evol.* 35:312-334.

Virtanen P, Gommers R, Oliphant TE, Haberland M, Reddy T, Cournapeau D *et al.* 2020. SciPy 1.0: Fundamental Algorithms for Scientific Computing in Python. *Nat Methods*. 17(3), 261-272.

von Schilcher F. 1976. The role of auditory stimuli in the courtship of *Drosophila melanogaster. Anim Behav*. 24:18-26.

Watanabe TK, Kawanishi, M. 1979. Mating preference and the direction of evolution in the *Drosophila. Science*. 205:906-907.

Wu C-I, Hollocher H, Begun DJ, Aquadro CF, Xu X, Wu M-L 1995. Sexual isolation in *Drosophila melanogaster*: A possible case of incipient speciation. *Proc Natl Acad Sci USA*. 92:2519-2523.

1092

Trait	FR Mean	ZI Mean	Pop. M-W P	FR Parent	ZI Parent	Par. M-W P	# QTLs	Effect range	Candidate genes
Bouts per Minute	7.00	7.05	1	6.24	7.83	0.0077	2	0.393 - 0.431	*dlg1*, *Gr10b*
Median Pulse Amplitude	0.100	0.078	0.088	0.097	0.063	7.00E-06	11	0.266 - 0.402	*Abd-B, Gr68a, mir-274, mir-285, mir-956, ple*
Median Pulse Train Length	1.16	1.09	0.161	1.07	1.16	0.0054	1	0.863	none
Median Sine Amplitude	0.177	0.171	0.600	0.19	0.14	0.0007	0	n/a	n/a
Median Sine Train Length	0.806	0.892	0.133	0.78	0.94	0.0313	5	0.499 - 0.747	*ss*
Mode Pulse Carrier Freq.	200	203	0.230	212	199	0.0140	1	0.270	none
Mode Sine Carrier Freq.	289	291	0.887	298	292	0.0026	0	n/a	n/a
Null to Sine Trans. Prob.	0.0039	0.0040	0.962	0.003	0.005	0.0008	1	0.430	*btv, CheB42a, Gr33a, Gr39a, Gr43a, Gr47a, jhamt, lig, Pal1, ppk25*
Slow to Total Pulses	0.745	0.813	0.007	0.745	0.833	0.0001	1	0.423	*ana1, BRWD3, Cad96Ca, CCAP-R, CG12290, CG13623, CG13654, CG31437, CG6432, CG6607, Dis3,* [E(spl) gene cluster]*, fid, Fur1, gro, jar, mld, Nf1, ppk15, Rrp5, slo, to*

1093

1094 **Table 1: Summarized Results for Mapped Traits.** Outcomes of population comparisons, RIL parental strain comparisons,
1095 and QTL mapping are listed for one trait with clear evidence of population differentiation (Slow to Total Pulses, bottom row)
1096 and eight other traits differing between RIL parental strains. FR and ZI indicate the France and Zambia population samples,
1097 from which multiple inbred strains were studied. “MW-P” indicates Mann-Whitney U Test p-values, presented for both the

population and parental strain comparisons. The range of QTL effect size point estimates (proportion of parental strain difference explained) among each trait's significant QTLs is presented; however, we note that some estimates for multi-QTL traits are likely to be inflated by linkage to other QTLs. Candidate genes based on functional considerations (see Materials and Methods) are listed for each trait. Genes listed for the trait "Slow to total pulses" additionally include others that fell within population genetic statistic outlier windows (Table S8, S9; Materials and Methods). More detailed results, including additional gene annotations, are provided in Tables S7, S8, and S9.

1104 FIGURES

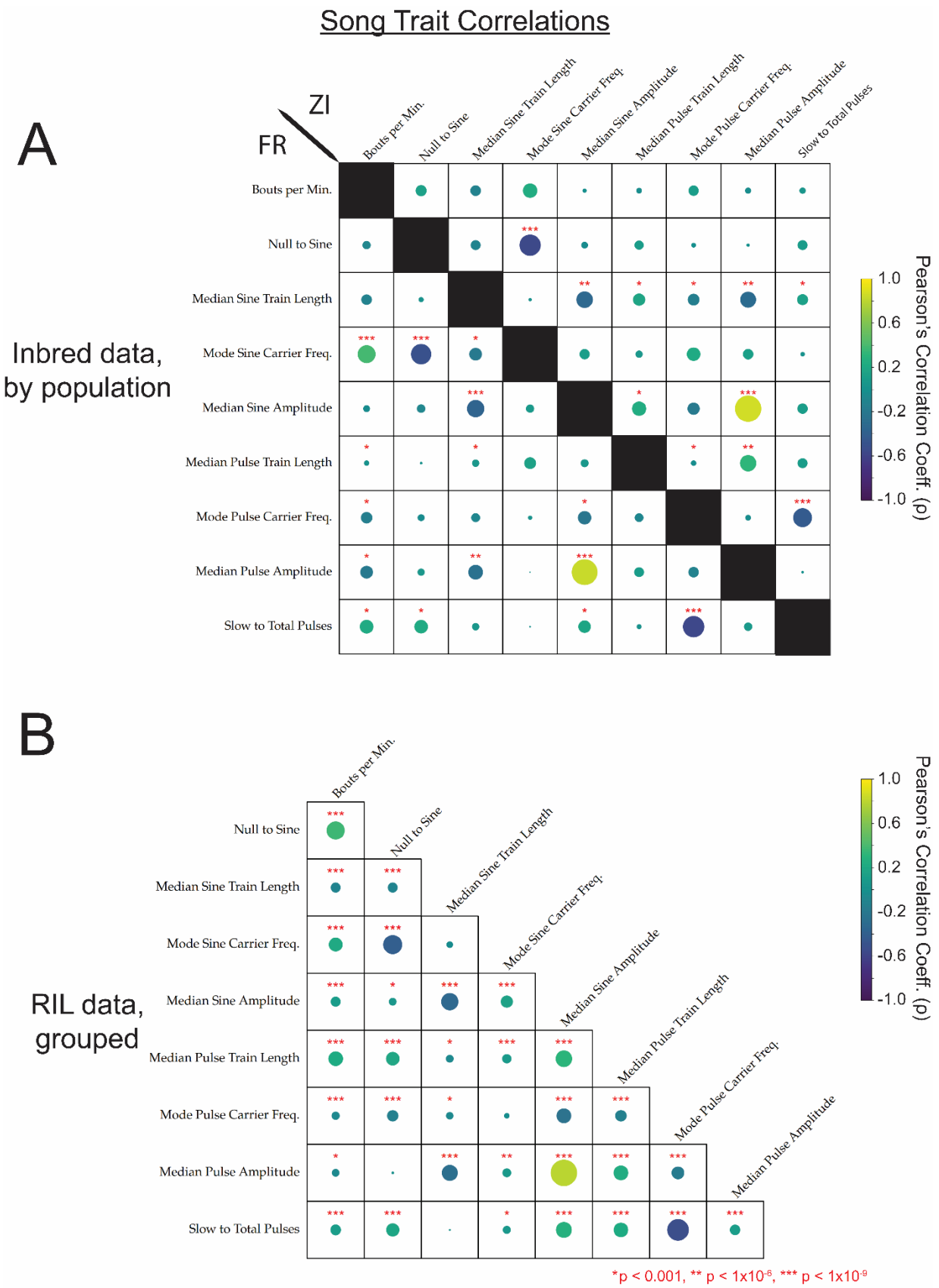
Song Trait Correlations
A
ZI
FR
Bouts per Min.
Null to Sine
Median Sine Train Length
Mode Sine Carrier Freq.
Median Sine Amplitude
Median Pulse Train Length
Mode Pulse Carrier Freq.
Median Pulse Amplitude
Slow to Total Pulses
Inbred data, by population
Pearson's Correlation Coeff. (ρ)
1.0
0.6
0.2
-0.2
-0.6
-1.0
B
RIL data, grouped
*p < 0.001, ** p < 1x10-6, *** p < 1x10-9

1105

1106 **Figure 1***: Correlation analysis between traits mapped from male song recordings reveals*
1107 *several positively and negatively correlated traits*. **A.** Correlations among inbred strains,
1108 divided by population (France bottom-left, Zambia top-right). **B.** Correlations among RILs.
1109 In all data sets, the strongest positive correlation was between pulse and sine amplitude
1110 traits. Circle size indicates the relative strength of significance in Pearson's (r) covariance
1111 between traits, where the presence of a circle indicates minimally a p-value of $p < 0.05$,
1112 and correlations with an estimated multiple-testing corrected significant p-values of $p <$
1113 1.0×10^{-3}, $p < 1.0 \times 10^{-6}$, and $p < 1.0 \times 10^{-9}$ are denoted with asterisks (*, **, and ***,
1114 respectively).
1115

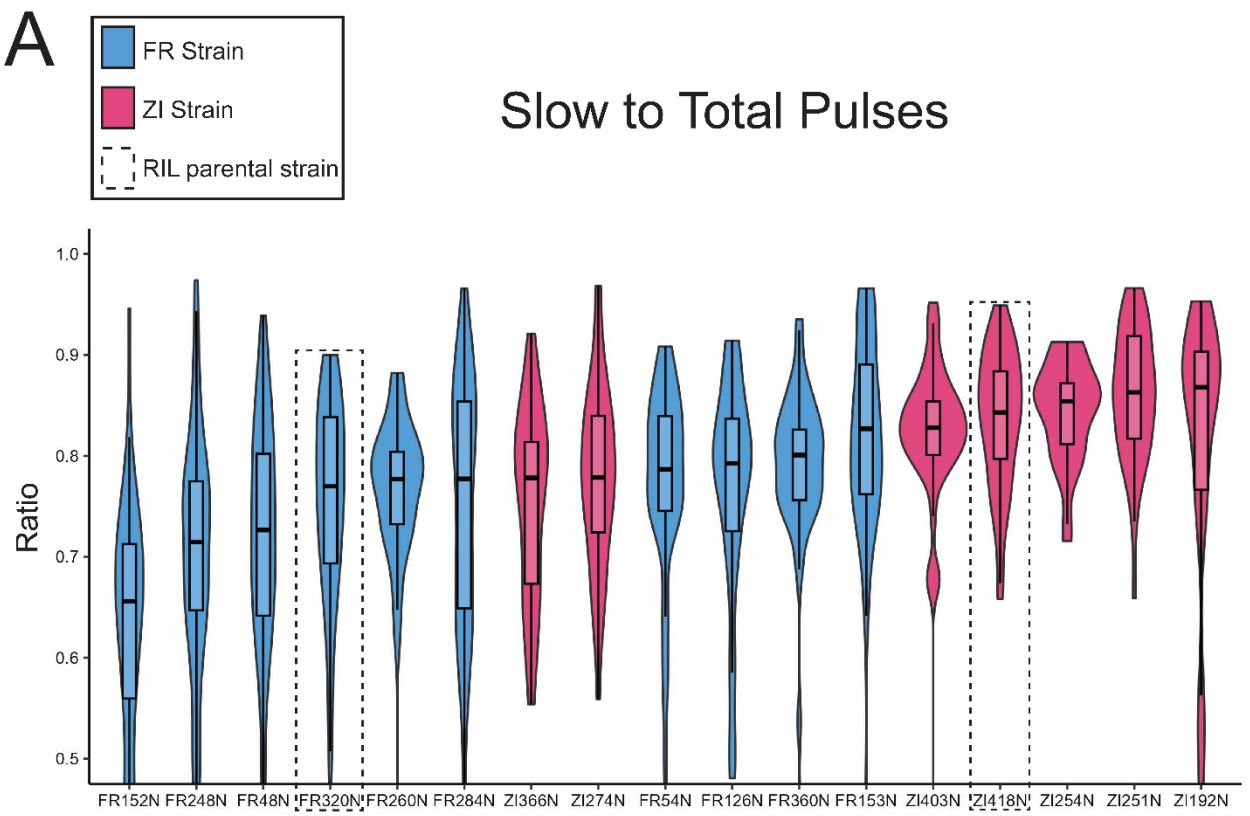
A
FR Strain
ZI Strain
RIL parental strain
Slow to Total Pulses
Ratio
1.0
0.9
0.8
0.7
0.6
0.5
FR152N FR248N FR48N FR320N FR260N FR284N ZI366N ZI274N FR54N FR126N FR360N FR153N ZI403N ZI418N ZI254N ZI251N ZI192N

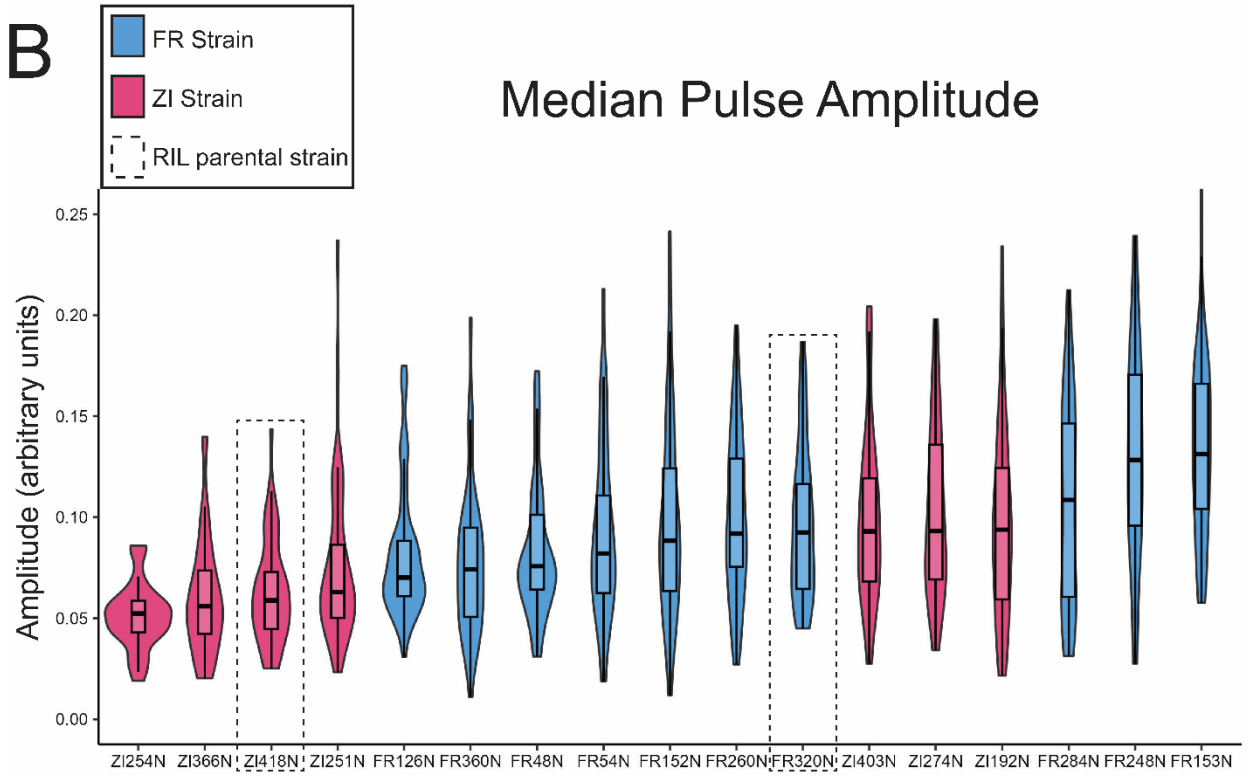
B
FR Strain
ZI Strain
RIL parental strain
Median Pulse Amplitude
Amplitude (arbitrary units)
0.25
0.20
0.15
0.10
0.05
0.00
ZI254N ZI366N ZI418N ZI251N FR126N FR360N FR48N FR54N FR152N FR260N FR320N ZI403N ZI274N ZI192N FR284N FR248N FR153N

1116

1117 **Figure 2**: *Zambia and France D. melanogaster males display differences in pulse mode*
1118 *preference (slow to total pulses) and in pulse amplitude.* Violin and boxplots for France
1119 (Blue) and Zambia (Red) males are displayed, with the middle line in boxplots
1120 representing median values, and inbred strains ordered by those median values. Parental
1121 strains used in the establishment of the RIL panel are highlighted by dotted boxes. The
1122 pairwise differences in both traits between parental strains is of similar magnitude and
1123 direction to that of the population trend, suggesting that some of the genetic variation
1124 contributing to phenotypic differences between populations may be represented among
1125 the RIL panel.

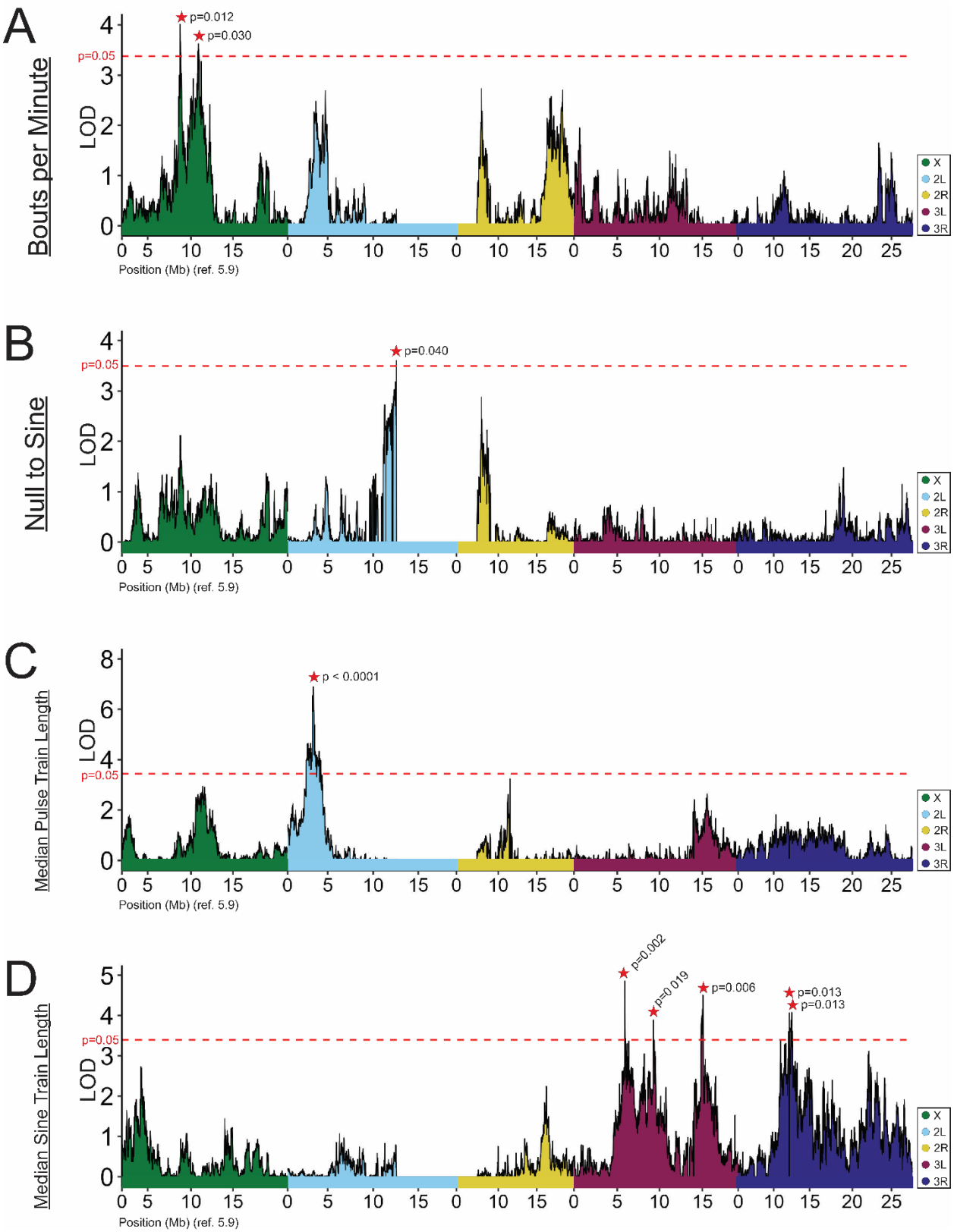
A
Bouts per Minute
p=0.012
p=0.030
p=0.05
LOD
Position (Mb) (ref. 5.9)
X
2L
2R
3L
3R
B
Null to Sine
p=0.040
p=0.05
LOD
Position (Mb) (ref. 5.9)
C
Median Pulse Train Length
p < 0.0001
p=0.05
LOD
Position (Mb) (ref. 5.9)
D
Median Sine Train Length
p=0.002
p=0.019
p=0.006
p=0.013
p=0.013
p=0.05
LOD
Position (Mb) (ref. 5.9)

1126

1127 **Figure 3**: *Traits associated with the amount and type of song map to unique QTLs*. The
1128 number of bouts per minute (A) mapped to a pair of nearby QTLs on the X chromosome
1129 - the only X-linked QTLs detected in this study. The probability of initiating sine song ("Null
1130 to Sine") (B) and the median length of pulse trains (C) mapped to single QTLs. In contrast,
1131 the median length of sine trains displayed a more polygenic basis, with multiple QTLs
1132 across both arms of chromosome 3, and distinct peaks from the pulse song counterpart
1133 of this trait (D). LOD values are plotted against *D. melanogaster* genome (release 5.9)
1134 positions, where color denotes chromosome arm. Genome-wide significance thresholds
1135 of LOD values corresponding to p = 0.05 for each scan are displayed as dashed lines.
1136 Significant peaks are denoted with a red star, with p-values noted. Further characteristics
1137 of each QTL are given in Table S7.

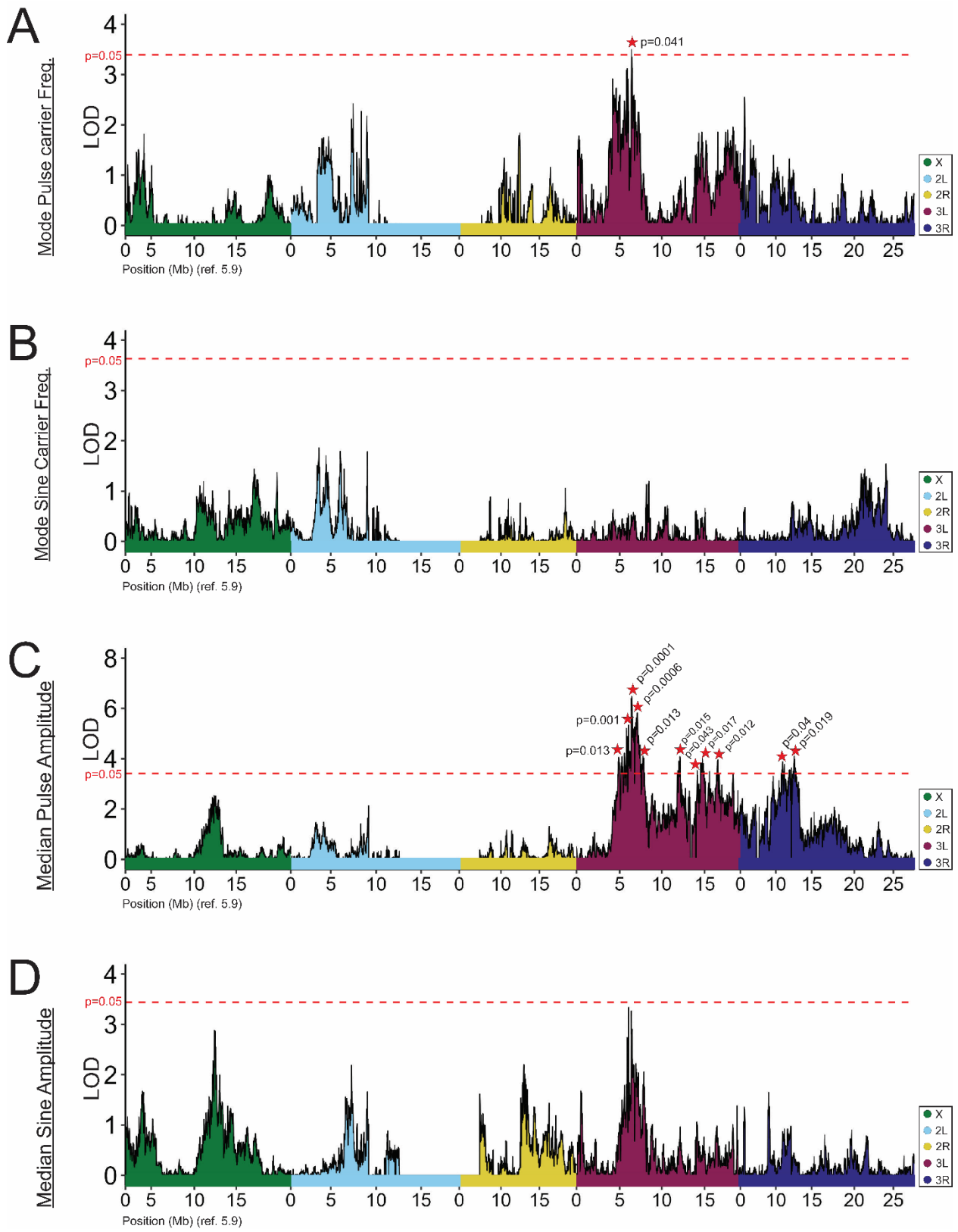
A
Mode Pulse carrier Freq.
LOD
p=0.05
p=0.041
Position (Mb) (ref. 5.9)
X
2L
2R
3L
3R
B
Mode Sine Carrier Freq.
LOD
p=0.05
Position (Mb) (ref. 5.9)
C
Median Pulse Amplitude
LOD
p=0.05
p=0.0001
p=0.0006
p=0.001
p=0.013
p=0.013
p=0.015
p=0.043
p=0.017
p=0.012
p=0.04
p=0.019
Position (Mb) (ref. 5.9)
D
Median Sine Amplitude
LOD
p=0.05
Position (Mb) (ref. 5.9)

1138

1139 **Figure 4**: *Traits associated with sine and pulse song qualities map to unique autosomal*
1140 *QTLs.* Both pulse (A) and sine (B) song amplitude and carrier frequencies were distinct
1141 between RIL parental strains, and map to unique QTLs. The only instance of partially
1142 overlapping QTL peaks was a region on chromosome 3R, overlapping QTLs for pulse
1143 amplitude (C) and sine train length (D), while the QTL for pulse carrier frequency was
1144 nearby, as was the nearly significant peak for sine amplitude. LOD values are plotted
1145 against *D. melanogaster* genome (release 5.9) positions, where color denotes
1146 chromosome arm. Genome-wide significance thresholds of LOD values corresponding to
1147 p=0.05 are displayed as dashed lines. Significant peaks are denoted with a red star, with
1148 p-values noted. Further characteristics of each QTL are given in Table S7.

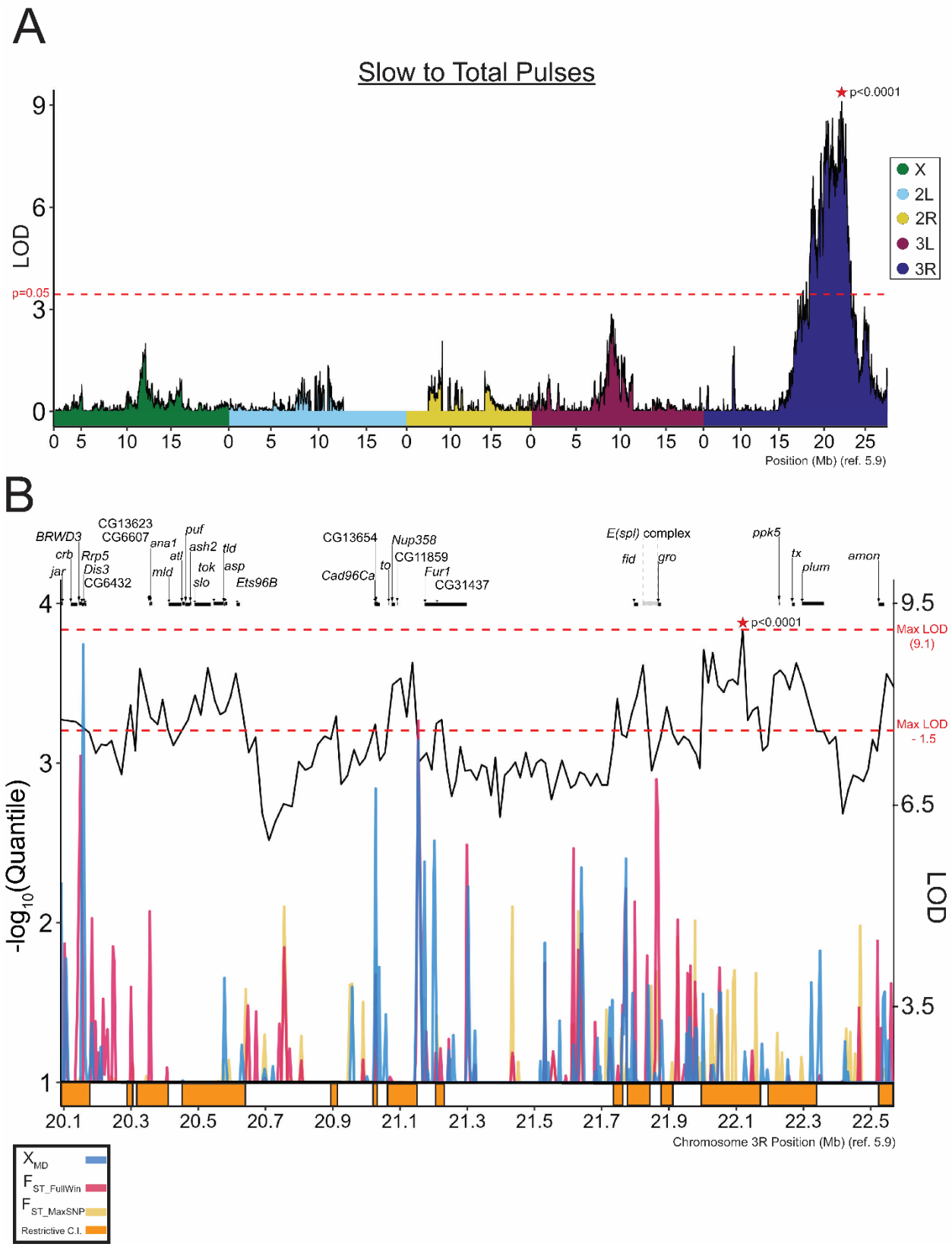
A
Slow to Total Pulses
p<0.0001
LOD
p=0.05
X
2L
2R
3L
3R
Position (Mb) (ref. 5.9)
B
BRWD3
crb
jar
Rrp5
Dis3
CG6432
CG13623
CG6607
ana1
mld
atl
puf
ash2
tok
slo
tld
asp
Ets96B
CG13654
Cad96Ca
to
Nup358
CG11859
Fur1
CG31437
E(spl) complex
fid
gro
ppk5
tx
plum
amon
p<0.0001
Max LOD (9.1)
Max LOD - 1.5
-log10(Quantile)
LOD
Chromosome 3R Position (Mb) (ref. 5.9)
XMD
FST_FullWin
FST_MaxSNP
Restrictive C.I.

1151 **Figure 5:** *Pulse mode preference maps to a single strong effect QTL, with potentially*
1152 *relevant genes indicated by functional annotation and population genetic analysis.* (A)
1153 QTL mapping of the quantitative trait "slow to total pulses" in song reveals a single strong
1154 QTL on chromosome 3R with a complex LOD landscape. All features of this plot are as
1155 described for Figures 3 and 4. (B) Negative log quantile values for $F_{ST_FullWin}$ (Red),
1156 F_{ST_MaxSNP} (yellow), and χ_{MD} (blue) reveal genomic regions with elevated population
1157 differentiation quantile values, sometimes overlapping peak LOD windows. $-\log_{10}$ quantile
1158 values on the left *y*-axis begin at 1.00 to better visualize outlier windows. Window LOD
1159 scores are represented as a black line (right *y*-axis). Restrictive confidence intervals are
1160 represented as orange boxes under the *x*-axis. The QTL peak's maximum LOD score
1161 and the (MaxLOD – 1.5) threshold are displayed as dashed red lines across the y-axis,
1162 with the latter value representing a threshold for restrictive Ci inclusion. We find an
1163 aggregation of more differentiated genomic sites within restrictive QTLs around 3R:21.75-
1164 22.25 Mb. This genomic region has been previously implicated in courtship behavior
1165 (Moehring & Mackay 2004). Further gene annotation details are available in Table S8**.**